



UNIVERSITY OF LEEDS

This is a repository copy of *Flow behaviour of grains through the dosing station of spacecraft under low gravity environments*.

White Rose Research Online URL for this paper:
<http://eprints.whiterose.ac.uk/116757/>

Version: Accepted Version

Article:

Antony, SJ orcid.org/0000-0003-1761-6306, Arowosola, B, Richter, L et al. (2 more authors) (2017) Flow behaviour of grains through the dosing station of spacecraft under low gravity environments. *Journal of Aerospace Engineering*, 30 (6). ISSN 0893-1321

[https://doi.org/10.1061/\(ASCE\)AS.1943-5525.0000789](https://doi.org/10.1061/(ASCE)AS.1943-5525.0000789)

© 2017, American Society of Civil Engineers (ASCE). This is an author produced version of a paper published in *Journal of Aerospace Engineering*. Uploaded in accordance with the publisher's self-archiving policy

Reuse

Unless indicated otherwise, fulltext items are protected by copyright with all rights reserved. The copyright exception in section 29 of the Copyright, Designs and Patents Act 1988 allows the making of a single copy solely for the purpose of non-commercial research or private study within the limits of fair dealing. The publisher or other rights-holder may allow further reproduction and re-use of this version - refer to the White Rose Research Online record for this item. Where records identify the publisher as the copyright holder, users can verify any specific terms of use on the publisher's website.

Takedown

If you consider content in White Rose Research Online to be in breach of UK law, please notify us by emailing eprints@whiterose.ac.uk including the URL of the record and the reason for the withdrawal request.



eprints@whiterose.ac.uk
<https://eprints.whiterose.ac.uk/>

1 **Flow behaviour of grains through the dosing station of spacecraft under low gravity**
2 **environments**

3
4 S. Joseph Antony*¹, Babatunde Arowosola², Lutz Richter³, Tulegen Amanbayev⁴ and Thabit
5 Barakat⁵

6
7 ¹Associate Professor, School of Chemical and Process Engineering, University of Leeds,
8 Leeds, LS2 9JT, UK. E-mail: S.J.Antony@leeds.ac.uk

9 ²Research Assistant, School of Chemical and Process Engineering, University of Leeds,
10 Leeds, LS2 9JT, UK. E-mail: pm10bca@leeds.ac.uk

11 ³Project Manager, OHB System AG, Manfred-Fuchs-Str. 1, 82234,
12 Weßling/Oberpfaffenhofen, Munich, Germany. E-mail: lutz.richter@ohb.de

13 ⁴Professor, Department of Mathematical Methods and Simulation, Tauke Khan Avenue, 5,
14 Southern-Kazakh State University, Shimkent, 160012, Kazakhstan. E-mail:
15 tulegen_amanbaev@mail.ru

16 ⁵Professor, Department of Physics and Astronomy, College of Science, King Saud University,
17 PO Box 2455, Riyadh, Saudi Arabia. E-mail: tbarakat@ksu.edu.sa

18 * Corresponding author: Tel.: ++44 (0)113 3432409; Email: S.J.Antony@leeds.ac.uk

19
20 **ABSTRACT**

21 For the design of the grain-processing stations of spacecrafts, such as EXOMARS 2020,
22 reliable estimates are required on the internal and bulk flow characteristics of granular media
23 under the low gravitational environments. Using theoretical and computational modelling, here
24 we present results on the generic flow behaviour of granular materials through flow channels
25 under different gravity levels. For this, we use three approaches, viz., (i) a simple one-
26 dimensional discrete layer approach (DLA) based on hybrid-Lagrange continuum analysis (ii)
27 three dimensional Kirya structural continuum model and (iii) three dimensional discrete
28 element modelling (DEM). Each model has its merits and limitations. For the granular simulant
29 considered here, a good level of agreement is obtained between the results of Kirya model and
30 DEM simulations on the flow properties of the grains. Some qualitative comparisons are also
31 reported favourably on the flow characteristics of grains between the results of the experimental
32 parabolic flight campaign and the DEM simulations. The theoretical and DEM simulations
33 presented here could help to minimise relying on the complex experimental programmes, such
34 as the parabolic flight campaign, for evaluating the processing behaviour of grains under low
35 gravitational environments in future.

36
37
38
39
40
41
42
43
44
45
46
47
48
49
50
51
52
53
54
55
56
57
58
59
60

INTRODUCTION

Space agencies of the world conduct extraterritorial ground exploration operations to explore human life beyond the earth. For example, the European Space Agency (ESA) aims to launch the EXOMARS rover mission to Mars in 2020, which involves operating a rover for the subsurface soil sampling and analysis. Using several electro-mechanical systems within the rover, samples acquired would be mechanically processed and dispensed to different instruments. In the design of the grain processing stations of such spacecrafts, a key requirement is understanding the flow behaviour of granular materials under low gravitational environments (Squyres et al. 2004; Yen et al. 2005; Antony et al. 2016).

Granular materials consist of discrete grains (Duran 1999). Micromechanical behaviours of granular materials have been studied extensively in the past, and they differ from that of conventional solids, liquids and gases states of matter (de-Gennes 1999; Schulze 2007; Lumay et al. 2009; Nguyen et al. 2014). For example the microscopic origin of shear strength is attributed to the contribution of a limited group of contacts, referred to as strong contacts, which depend on their particle-scale properties (Antony 2007, Kruyt and Antony 2007). Recent experimental studies using Digital Particle Image Velocimetry (Albaraki and Antony 2014) provide information on how grain-scale properties influences on the flow behaviour of granular media at both micro and bulk scales under the earth gravity. However, such details are scarce in the literature for the low gravitational environments.

For simulating the processing characteristics of granular materials, DEM is used more commonly in the recent times (Cundall and Strack 1979). DEM models the interaction between contiguous grains as a dynamic process and the time step is advanced using an explicit finite

61 difference scheme (Cundall and Strack 1979). The method enables to predict both the
62 microscale (internal) and bulk scale mechanical characteristics of granular materials under
63 different loading and environmental conditions. So far, investigations on the mechanical
64 behaviour of granular materials are widely reported under the earth gravity conditions, but
65 relatively to a small extent under other gravitational conditions (Liu and Li 2010; Hofmeister
66 et al. 2009). Under the low-gravitational conditions, certain material properties such as the
67 cohesion of the grains could influence on the macroscopic flow properties relatively more with
68 that of the earth gravitational condition (Walton et al. 2007). This is due to potential changes
69 in the chemical activity of the grains under low gravitational environments. For example, the
70 lunar granular surfaces could be chemically more active and result more surface energy when
71 compared with the same mineralogy of the grains under the earth gravity (Walton et al. 2007).
72 This could also result the formation of the grains (or their agglomerates) in non-spherical
73 shapes. For simulating the mechanical behaviour of granular assemblies, some DEM studies
74 account for the non-spherical shape of the grains by considering them as a collection of
75 prolates, oblates (Antony and Kuhn 2005), or by fusing individual spheres to construct any
76 non-spherical shape of the grains (Walton and Braun 1993, Chung and Ooi 2007). Theoretical
77 analysis have been also reported in the past to determine the bulk flow properties of the grains,
78 for example using the simple Beverloo equation (Beverloo et al. 1961) comprising an empirical
79 correlation coefficient. Some studies (Chung and Ooi 2007) on the bulk flow rate of the grains
80 have reported that such predictions depend on the selection of the correlation coefficient. The
81 value of this correlation coefficient is not yet well defined to different terrestrial grains and
82 environments. Furthermore, Beverloo equation does not directly account for the inter-particle
83 friction of the grains (Beverloo et al. 1961).

84

85 In general, DEM simulations are computationally expensive, especially under the low gravity
86 conditions (Brucks et al. 2008). It would be desirable to evaluate the flow properties of grains
87 under the low gravity conditions using DEM and to compare the outcomes with relatively less-
88 expensive continuum approaches where feasible. The current research focuses on this by
89 evaluating the influences of grain-scale properties of the non-cohesive grains on their flow
90 properties under a range of gravitational environments, including that of less than the earth
91 gravity (low gravity). The study involves applying simple theoretical models and more
92 extensive discrete element modelling depending on different scenarios.

93

94 **THEORETICAL AND NUMERICAL METHODS**

95 The theoretical methods adopted here are of two types namely: Discrete Layer Approach
96 (DLA) by considering one-dimensional granular flow through a two-dimensional hopper, and
97 the three-dimensional Kirya's structural model. Results from the three-dimensional DEM
98 simulations are compared with corresponding Kirya's structural model at later stages.

99 **Theoretical Analysis using discrete layer approach (DLA)**

100 In the DLA approach, the particles are represented as discrete layers (Fig. 1). Hence this comes
101 with the simplification, in which instead of considering individual particles as such, group of
102 particles are represented as thin discrete layers of height h , and each layer would represent the
103 collective flow behaviour of particles within them based on Lagrange approach. The flow
104 geometry is two dimensional in which the flow of grains occurs along the vertical axis (Fig.1).
105 For a given steady-state flow rate Q of the grains through the hopper of a given throat angle,
106 the model helps to estimate the discharge completion time, the position of the particles with
107 time (Lagrange coordinate) and the velocity of granular layers within the hopper. Though the
108 model does not explicitly take into account the gravity term in the final equations, it helps to

109 evaluate the flow trajectories of the layers and the completion time required to empty flow
 110 funnels under a steady flow rate ($Q \text{ m}^2/\text{s}$) condition by assuming that when other conditions
 111 are identical, proportionately higher steady flow rates corresponds to flow of materials under a
 112 relatively high level of gravity and vice versa.

113 For this, it is assumed that the granular material is incompressible – an assumption that in fact
 114 is not fully valid for planetary regolith. We select an elementary volume of discrete granular
 115 layer which is also called as a ‘large particle element’ with thickness $h \ll H$ (Fig. 1). The
 116 Lagrange coordinate, ξ is employed as the initial coordinate of centre of the large particle
 117 element (elementary volume of media) as shown in Fig. 1. Hence that the boundary conditions
 118 are:

$$119 \quad \begin{cases} t = t_0 : y = \xi \\ t > t_0 : y = f(\xi, t) \end{cases} \quad (1)$$

120 where y is the Euler coordinate of centre of large particle element.

121 It is necessary to find the law of motion of the elementary volume:

$$122 \quad y = f(\xi, t) \quad (2)$$

123 For incompressible media, the area of elementary volume (S) will be constant. Using this
 124 condition together with the geometrical dimensions of the hopper, the following relations are
 125 obtained to develop computational schemes for the subsequent analysis:

$$126 \quad y = \frac{h}{h_1} \left(\xi + \frac{a}{2 \tan \alpha_1} \right) - \frac{a}{2 \tan \alpha_1} \quad (3)$$

$$127 \quad h_1 = (h_{11} - h_{12}) / \tan \alpha_1, \quad \alpha_1 = \alpha / 2 \quad (4)$$

128 where, h_1 is the thickness of the particle element at time t (Fig.1) and h_{11} , h_{12} are defined as

$$129 \quad h_{11} = \sqrt{\left(\xi \tan \alpha_1 + \frac{a}{2} + \frac{h}{2} \tan \alpha_1 \right)^2 - (t - t_0) Q \tan \alpha_1} \quad (5)$$

$$h_{12} = \sqrt{\left(\xi \tan \alpha_1 + \frac{a}{2} - \frac{h}{2} \tan \alpha_1\right)^2 - (t - t_0) Q \tan \alpha_1} \quad (6)$$

131

132 **Analysis of factors influencing the granular flow using DLA**

133 Two different heights of the container fill (H) is considered in this study, viz., 0.2m (case1-
 134 $\xi=0.2$) and 0.3m (case2- $\xi=0.3$) and various values of flow rate Q. Unless mentioned otherwise,
 135 the size of the slit 'a' is kept as 0.1m and the hopper angle α as $\pi/3$ (Fig. 1). However at later
 136 stages, the analysis has been extended to different combinations of a and α to understand their
 137 individual roles on the characteristics of granular flow.

138 At first, the theoretical results were analysed by tracking the motion/position 'y' of the topmost
 139 thin discrete layer (h=0.001 m, Fig. 1) with respect to time as presented in Fig. 2. T_{empty} , which
 140 is the emptying time (i.e., time required to complete the flow of granular material through the
 141 container. This would correspond to the time when y tends to zero). Hence, the value of T_{empty}
 142 can be extracted from Fig. 2 and presented in Fig. 3 as a function of granular flow rate. From
 143 these results, it is evident that the time required to empty the container (T_{empty}) decreases for an
 144 increase in the flow rate as one could expect (Schulze and Schwedes 1990). However, From
 145 Fig. 3, it is interesting to note that this decrease in T_{empty} occurs at a rapidly decreasing rate for
 146 the flow rate up to about 0.003 m²/s, and this trend tends to diminish beyond a flow rate of
 147 0.003 m²/s for both cases of the container with different heights ($\xi=0.2$ and 0.3). Hence, in
 148 general, the low gravity effects are more likely to slow down the flow of grains in the selected
 149 dosing funnel (hopper) geometry especially when the processing flow rate is relatively low
 150 (approximately the minimum cut off flow rate is 0.003 m²/s).

151 The influence of the hopper angle α (Fig. 1) on the granular flow behaviour is analysed for a
 152 typical value of flow rate 0.003 m²/s. As discussed above, the corresponding time required to
 153 empty the container T_{empty} is also calculated and presented in Fig. 4. It is evident that the time

154 required to empty the containers due to granular flow increases for increase in the hopper angle.
 155 This is qualitatively in agreement with the recent experimental studies though conducted under
 156 the earth gravity (Antony and Albaraki 2014) in which increase in the hopper angle resulted an
 157 increase in the completion time of the granules. This behaviour is more noticeable for the
 158 hopper throat angle between $\pi/2$ and $\pi/3$, as well as more significantly when the height of the
 159 container is relatively high ($\xi=0.3$). Hence for designing the dosing container, hopper throat
 160 angle of less than $\pi/3$, where feasible, is desired from the point of view of maintaining good
 161 flowability of the grains from the container, especially when the height of the container is more
 162 than 0.2m ($\xi>0.2$). This could be attributed to the favourable direction of the resultant velocity
 163 of the grains during the flow. Experimental granular flow studies conducted using Digital
 164 Particle Image Velocimetry (DPIV) under the earth gravitational condition (Antony and
 165 Albaraki 2014) have also shown that, for a smaller hopper angle (e.g. $\pi/6$), the direction of the
 166 resultant velocity of the grains align along the direction of the gravity almost throughout the
 167 hopper and favours a uniform flow. This trend diminished significantly in the case of a higher
 168 hopper angle (e.g. $\pi/2$) and resulted a non-uniform funnel flow (Antony and Albaraki 2014)
 169 with a relatively more time to complete the flow through the hopper.

170 The DLA model was also used to monitor the velocity profile of the particle during granular
 171 flow in the hopper. The velocity of the particle can be evaluated as:

$$172 \quad v = \frac{dy}{dt} = -\frac{1}{2} \frac{hQ}{h_1 h_{11} h_{12}} \{ \xi \tan \alpha_1 + a/2 \} \quad (7)$$

173 Fig. 5 shows the typical velocity distribution of the particle inside the hopper ($\xi=0.3$, $\alpha=\pi/3$,
 174 $a=0.1$ m). The velocity is at a maximum at the exit of the hopper ($y=0$) during granular flow in
 175 agreement with other studies (Cox and Hill 2005). The above presented DLA analysis helps
 176 to evaluate some useful flow characteristics of granular media in a simple manner. However,

177 for studying more rigorous three-dimensional flow of grains under the low gravitational
178 environments, the following analysis is presented.

179 **Analysis of the discharge rate of grains under low gravity using Kirya's structural**
180 **continuum model**

181 Here, the aim is to study on when other conditions are identical between different cases, to
182 what extent the steady state granular flow rate (Q) of frictional grains (inter-particle friction)
183 varies if the gravitation field of the container is different from that of earth gravity g_0 (reference
184 gravity level). For selected cases, DEM simulations are reported later for the purpose of
185 comparisons. Such an analysis would provide beforehand indications of the variations in the
186 flow properties when actual experiments are conducted to corresponding conditions in the
187 parabolic flight campaign in the future.

188 The theoretical analysis was performed based on Kirya's three-dimensional structural
189 continuum model and the details can be found elsewhere (Kirya 2009). As the original
190 description of this model is in Russian, and for the benefit of the wider audience of this journal,
191 we describe the key developments of Kirya's model here. In brief, the flow trajectories of the
192 grains inside a smooth hopper is divided into different zones A-E (Fig.6a). In zone A, the
193 granular medium particles are interconnected and move at a low speed parallel to the walls of
194 the hopper. In zone B, the particles slide relative to each other, and their trajectories are bent
195 towards the axis of the hopper. In zone C, the granular particles form movable vaults moving
196 downward, while the particle velocities increase substantially, and their trajectories approach
197 vertical lines. In the zone of collapse (mixing) D, connections between particles are destroyed,
198 while they are in continuous chaotic motion, colliding with each other, and their speed increases
199 due to gravity. In zone E, the particles are stationary (Kirya 2009). In the present case, the
200 objective is to focus on the exit flow rate of the grains from the hopper. Hence the description
201 of exit flow zone-D bounded by a parabola (Fig. 6b) is considered here. In this zone, the

202 granular particles collide with other particles continuously and in a chaotic movement. The
 203 grains are in a free disperse state and their movement can be described by the Navier Stokes
 204 equations for granular materials (Kirya 1999, Kirya 2009). The boundary between the dynamic
 205 arc C, and the exit flow zone D could be represented in the form of a parabola (Fig. 6b) in the
 206 following form (Kirya 2009):

$$207 \quad y = h_c \left[1 - \left(\frac{2x}{a} \right)^2 \right] \quad (8)$$

208 Where h_c is the height of parabola, which can also be defined as:

$$209 \quad h_c = \frac{a}{4} \frac{1 + \sin\varphi}{\cos\varphi} = \frac{a}{4} \left(\mu + \sqrt{1 + \mu^2} \right) \quad (9)$$

$$210 \quad \mu = \tan\varphi \quad (10)$$

211 In which μ is the coefficient of inter-particle friction, φ is the angle of internal friction and a is
 212 the size of the opening (Fig.6b).

213 The parabola shown in Fig. 6b can be substituted by linear sections. The equation of the linear
 214 boundary has the following form:

$$215 \quad y = h_c \left[1 - \frac{2|x|}{a} \right] \quad (11)$$

216
 217
 218 in which $-a/2 \leq x \leq a/2$. By using Bernoulli equation to the cross-sections 1-1 and 2-2 for
 219 considered triangle, we obtain

$$220 \quad y_1 + \frac{p_1}{\gamma} + \frac{v_1^2}{2g} = y_2 + \frac{p_2}{\gamma} + \frac{v_2^2}{2g} + \zeta \frac{v_2^2}{2g} \quad (12)$$

221 where y_1, y_2 are levels of sections 1-1 and 2-2 respectively; p_1, p_2 are normal tensions at the
 222 points of interceptions of sections 1-1 and 2-2 with lateral sides of the triangle; v_1, v_2 are
 223 corresponding velocities of particles at the above said points; g is gravitational acceleration; γ

224 is the unit weight of granular material; ζ is Darcy-Weissbakh coefficient of local loss
 225 characterizing the loss of mechanical energy of granular flow by collisions between particles
 226 (Shterenliht, 1984). By substituting $y_1=y$, $y_2=0$, $p_1=0$, $p_2=0$, $v_1=v_d$, $v_2=v_e$ in to Eq. (12)
 227 and after transformations, the value of velocity of particles of granular material on the chink
 228 exit from the tank can be written as

$$229 \quad v_e = \frac{1}{\sqrt{1+\zeta}} \sqrt{2gy + v_d^2} \quad (13)$$

230 Where v_d is the velocity of particles at a point of intersection and can be expressed as

$$231 \quad v_d = \sqrt{\frac{2g\sigma_2}{\gamma}} \quad (14)$$

$$232 \quad \sigma_2 = \gamma \left(\frac{1}{\mu} + \mu - \sqrt{1 + \mu^2} \right) x \quad (15)$$

233 Substituting Eqs.(14) and (15) into Eq.(13) results as:

$$234 \quad v_e = \frac{1}{\sqrt{1+\zeta}} \sqrt{2g \left(y + \frac{\sigma_2}{\gamma} \right)} \quad (16)$$

235 The volume expenditure of granular material per unit length through the chink is defined as:

$$236 \quad Q = \int_{-a/2}^{a/2} v_e dx \quad (17)$$

$$237 \quad Q = \frac{2}{3} a^{3/2} \sqrt{g} \frac{1}{\sqrt{1+\zeta}} \frac{K_1^{3/2}}{K_1 - \chi'} \left[1 - \left(\frac{\chi'}{K_1} \right)^{3/2} \right] \quad (18)$$

238 where,

$$239 \quad K_1 = \frac{1}{2} \left(\mu + \sqrt{1 + \mu^2} \right) \quad (19)$$

$$240 \quad \chi' = \mu + \frac{1}{\mu} - \sqrt{1 + \mu^2} \quad (20)$$

241 The coefficient of loss, ζ at the movement of granular material in the zone of flow out can then
 242 be defined as

$$243 \quad \zeta = K_2 \frac{\kappa^2 d^2 h_c}{a^3} \quad (21)$$

244 where K_2 is unit dimensionless coefficient dependent on the conditions of flow out from the
245 tank (≈ 1); d is the diameter of the particle (average size in the analysis); a is width of the exit
246 flow channel in zone D; and κ ($=10$) is the kinetic coefficient which characterizes the loss of
247 mechanical energy flow by collisions between particles (Kirya 2009). The size of the opening
248 a is kept as 10mm (Fig.6b) for the analysis. Furthermore, from Eqs.(9) and (19) it follows that
249 $h_c = K_1 a/2$. Hence Eq.(21) can be written more generally as:

$$250 \quad \zeta = K_1 K_2 \frac{\kappa^2 d^2}{2a^2} \quad (22)$$

251
252 Using Eq.(18), the effects of friction coefficient on the flow properties (Nedderman 1992) of
253 grains (uniform grain size 100 μ m) are studied here under a range of gravity levels. The friction
254 coefficient was varied from 0.1 – 0.5 and gravity from 20– 200% of earth gravity and the results
255 are presented in Fig.7. In this, the flow rate (Q) under a given gravity level (g) is normalised
256 with respect to that of earth gravity condition (Q_0, g_0). The results show that the flow rate
257 increases with the gravity (Sun and Sankaran 2012). However this increase is more dominant
258 in the case of low frictional materials ($\mu \leq 0.3$) and under relatively high gravity ($g > g_0$). For
259 particles with friction coefficient greater than 0.3, interparticle friction does not have a
260 dominant effect on the granular flow rate under the low gravity environments ($g < g_0$).

261

262 **DEM modelling of gravity effects on flow rate (Q) of the grains**

263 The objective of this section is to evaluate the macroscopic flow rate Q of the sandstone grains
264 passing through a typical spacecraft flow channel of the grain-processing station using DEM
265 simulations. The results are also compared with corresponding continuum analysis using the
266 Kirya's continuum model as described in the previous section. DEM models the interaction
267 between individual grains as a dynamic process and the time advancement is based on
268 Newton's law of motion and using an explicit finite difference scheme (Cundall and Strack

269 1979). For more details of the DEM simulation methodology for low gravity levels, the readers
270 could refer to the work of Nakashima et al. (2011), though their work pertains to two-
271 dimensional conditions for studying the angle of repose of granular materials post-flowing
272 through hopper under low gravity conditions. However, in the present paper, the DEM
273 simulations are presented for three-dimensional conditions. The dimensions of the three
274 dimensional flow channel (hopper) are presented in Fig.8. Discrete spherical particles (normal
275 size distribution with an average size of $100\mu\text{m}$, and the ratio of maximum to minimum size of
276 the grains=1.6) were initially created in a random static packing inside the hopper assembly
277 with typical material properties of sandstone grains and hopper (Table 1). After generating the
278 initial random assembly of the grains inside the hopper geometry to the required initial porosity,
279 they were allowed to flow through by opening the throat of the hopper.

280

281 Fig.9 shows the time required to empty the sandstone grains from the hopper under different
282 gravity levels. This presents on the strong influence of gravity plays on the flow characteristics
283 of the grains, i.e., at the low gravity levels (about $g < 0.6g_0$) the flow of the grains is significantly
284 slow when compared with that of earth gravity. The emptying time tends to be inversely
285 proportional to the level of gravity. Similar generic trends are also reported earlier in the
286 experimental investigation using grains passing through the hourglass (Le Pennec et al. 1995,
287 Hofmeister et al. 2009).

288

289 To understand on the extent to which the DEM simulation results agree with continuum
290 analysis under different gravity levels, Kirya's model (as described in the previous section) is
291 used for the geometrical conditions and material properties used in the present DEM
292 simulations. The average flow rate obtained from the DEM simulations is compared with the
293 flow rate obtained from the Kirya's model in Fig.10. Interestingly, a good level of agreement

294 is obtained between these results based on the two different approaches, especially when $g \leq g_0$.
295 This helps to assess the bulk flow rate of grains through the hopper flow devices under low
296 gravity more easily using the Kirya's model as DEM simulations are computationally more
297 expensive (Cundall and Strack 1979). However, DEM simulation data could give more
298 information on the internal and discrete behaviour of the grains inside the flow devices, which
299 is outside the scope of the current work.

300

301 The flow characteristics of sandstone using DEM is compared qualitatively with the
302 observations made from a parabolic flight test (Thomson, 1986) and presented in Fig.11. For
303 this, a preparatory experiment involved studying the mass flow of grains through the hopper,
304 and then to increase the gravity level rapidly to $2g_0$ to completely evacuate the grains quickly
305 (without any particles sticking to the wall surfaces to avoid potential contaminations). In this
306 case, flow of the sandstone material through the funnel geometry was observed and a
307 significant level of blockage of the grains occurred in the funnel under the lunar gravity level.
308 This was also quantified using corresponding DEM simulations (as described earlier). The
309 containment of the particles in the funnel was observed (Fig.11). Further tests were carried out
310 by simulating a $2g_0$ gravity environment with the remaining stuck in the hopper. Also, the
311 gravity environment of the experiment was suddenly increased to $2g_0$ level which completely
312 ejected the blocked grains and this agreed with the DEM simulation results as well. The total
313 mass of grains ejected from the funnel increased drastically under the $2g_0$ gravity environment
314 and within a short simulation time-steps, all the particles were discharged out of the hopper
315 (Fig. 11). However, further experimental studies are required to make detailed measurements
316 and their quantitative comparisons with the results based on the DEM and theoretical analysis,
317 although creating a long duration low-gravitational environmental for experimental testing is a
318 stiff challenge yet.

319

320 **CONCLUSIONS**

321 Both continuum and discrete approaches have been used in this study to understand the flow
322 characteristics of granular materials through flow geometries under different gravitational
323 environments. Though the DLA approach is the most simplest of all, it helps to evaluate the
324 dynamic nature of the grains such as the completion time of the flow under different
325 gravitational conditions. Furthermore, the results on the bulk flow properties under low
326 gravitational levels of the grains based on the Kirya's approach agreed well with that of the
327 DEM simulations. A simple continuum approach such as Kirya's model could help to estimate
328 the three dimensional flow behaviour of frictional grains more quickly unlike in the case of
329 DEM simulations, which involve a significantly high amount of computational time and
330 resources, especially for studying the low gravitational behaviour of granular materials. The
331 present analysis helps to estimate the granular flow measures at different gravity levels
332 including low gravity. The approaches outlined here could help to minimise using parabolic
333 flight campaigns (which are more expensive with respect to manpower, flight costs and
334 managing the risks) for evaluating the flow properties of cohesionless and frictional grains.
335 Further detailed studies are required and underway to understand on the internal mechanics,
336 physics and bulk dynamic flow characteristics of more realistic granular simulants, and suitable
337 mechanisms to enhance granular flow under the low gravitational environments.

338

339 **ACKNOWLEDGEMENT**

340 This Project was funded by the National Plan for Science, Technology and Innovation
341 (MAARIFAH), King Abdulaziz City for Science and Technology, Kingdom of Saudi Arabia,
342 Award Number (12-SPA2925-02).

343

344 **REFERENCES**

345 Albaraki, S. and Antony, S.J. (2014). “How does internal angle of hoppers affect granular
346 flow? – Experimental studies using digital particle image velocimetry.” *Pow.Tech.*, 268, 253–
347 260

348 Antony, S.J (2007). “Link between single-particle properties and macroscopic properties in
349 particulate assemblies: role of structures within structures.” *Phil. Trans. Roy. Soc. London*,
350 *Series: A.*, 365, 2879-2891.

351 Antony, S.J., Arowosola, B., Richter, L., Amanbayev, T., and Barakat, T. (2016). “Modelling
352 the flow behaviour of granular media through the dosing station of spacecraft under low
353 gravitational environments.” *ASCE Earth and Space Conference*, Orlando, USA, No.
354 1570207049

355 Antony, S.J. and Kuhn, M.R. (2005). “Influence of particle shape on the interplay between
356 contact signatures and particulate strength.” *Int. J. Solids Struct.*, 41, 5863-5870.

357 Beverloo, W. A., Leniger, H. A., and van de Velde, J. (1961). “The flow of granular solids
358 through orifices.” *Chem. Eng. Sci.*, 15, 260–269.

359 Brucks, A., Richter, L., Vincent, J. & Blum, J. (2008). “Effect of Reduced-Gravity Conditions
360 on the Flowability of Granular Media.” In: Binienda, K.W., ed. *Earth & Space 2008*,
361 California, USA. ASCE, 1-8

362 Chung, Y.-C., and Ooi, J. Y. (2008). “A study of influence of gravity on bulk behaviour of
363 particulate solid.” *Particuology*, 6, 467–474.

364 Cox, G. M. & Hill, J. M. (2005). “Some Exact Velocity Profiles for Granular Flow in
365 Converging Hoppers.” *Z. Angew. Math. Phys.* 56, 92-106.

366 Cundall, P. A., and Strack, O.D.L. (1979). “A discrete numerical model for granular
367 Assemblies.” *Geotech.*, 29(1), 47-65.

368 De-Gennes, P. G. (1999). “Granular Matter: A Tentative View.” *Rev. Mod. Phys.*, 71, S374-
369 382.

370 Duran, J. (1999). *Sands, Powders, and Grains: An Introduction to the Physics of Granular*
371 *Materials*. Berlin, Springer.

372 Hofmeister, P. G., Blum, J. and Heißelmann, D. (2009). “The Flow Of Granular Matter Under
373 Reduced-Gravity Conditions.” *AIP Conf. Proc.*, 1145:71-74

374 Kirya, R.V. (1999). “The kinetic approach to equations of flow of granular materials.” *News*
375 *of Dnepropetrovsk State University, Mechanics*, 2, 143-150 (in Russian)

376 Kirya, R.V. (2009). “The description of process of flow out of granular material from tank by
377 structural-mechanical models.” *Sys. Tech.*, 3(62) 3-19 (in Russian) (Available online:
378 st.nmetau.edu.ua/journals/62/1_a_ru.pdf)

379 Kruyt, N.P. and Antony, S. J. (2007). “Force, relative displacement and work networks in
380 granular media subjected to quasi-static deformation.” *Phy. Rev E.*, 75, 051308

381 Le Pennec, T., Ammi, M., Messenger, J. C., Truffin, B., Bideau, D. and Garnier, J. (1995).
382 “Effect of gravity on mass flow rate in an hour glass.” *Pow. Tech.*, 85, 279-281.

383 Liu, Y. and Li, G. (2010). “Numerical prediction of particle dispersions in downer under
384 different gravity environments.” *Chem. Eng.*, 158, 281-289.

385 Lumay, G., Dorbolo, S., and Vandewalle, N. (2009). “Compaction dynamics of a magnetized
386 powder.” *Phy. Rev E.*, 80, 041302.

387 Nakashima, H., Shimizu, H., Miyasaka, J., Ohdoi, K., Aoki, S., Kobayashi, T., and Shioji, Y.
388 (2011). “Determining the angle of repose of sand under low-gravity conditions using discrete
389 element method.” *Jl. Terramech.*, 48, 1, 17-26

390 Nedderman, R. M. (1992). *Statics and Kinematics of Granular materials*. Cambridge Univ
391 Press, Oxford, UK.

392 Nguyen, T. K., Combe, G., Caillerie, D. and Desrues, J. (2014). “FEM × DEM modelling of
393 cohesive granular materials: Numerical homogenisation and multi-scale simulations.” *Acta*
394 *Geophy.*, 62, 1109-1126.

395 Schulze, D. (2007). *Powders and Bulk Solids: Behaviour, Characterization, Storage and Flow*,
396 Springer Berlin Heidelberg.

397 Schulze, D. and Schwedes, J. (1990). "Storage and flow of bulk solids in silos and information
398 for planning new installations." *VGB-Kraftwerkstechnik (English version)*, 70, 665-669.

399 Shterenliht, D.V. (1984) *Hydraulics*, Koloss, Moscow (in Russian).

400 Squyres et al. (2004) "The Spirit Rover's Athena Science Investigation at Gusev Crater, Mars."
401 *Science*, 305(5685), 794 – 799

402 Sun, J. and Sankaran, S. (2012). "Radial hopper flow prediction using a constitutive model
403 with microstructure evolution." *Pow. Tech.*, 242, 81 - 85.

404 Thomson, W. (1986) *Introduction to space dynamics*, Dover, New York

405 Walton, O.R., Moor, C.P and Gill, K. S. (2007). "Effect of gravity on cohesive behaviour of
406 fine powders: implications for processing Lunar regolith." *Granu. Matt.*, 9, 353-363

407 Walton, O.R., and Braun, R.L. (1993). "Simulation of rotary-drum and repose tests for
408 frictional spheres and rigid sphere clusters." In: *Joint DOE/NSF Workshop on Flow of*
409 *Particulates and Fluids*, September 29 – October 1, Ithaca, NY (1993). (Available online:
410 www.grainflow.com)

411 Wang, L. P., Carey, V. P., Greif, R. and Abdollahian, D. (1990). "Experimental simulation and
412 analytical modelling of two-phase flow under zero-gravity Conditions." *Int. Jl. Multiph. Flow*,
413 16, 407-419.

414 Yen et al. (2005) "An integrated view of the chemistry and mineralogy of Martian soils."
415 *Nature*, 436, 49-54.

416
417
418
419
420

421 **Table 1.** Material properties used in the DEM simulations

wall normal stiffness = $1e8$ N/m	wall shear stiffness = $1e8$ N/m
grain normal stiffness = $1e8$ N/m	grain shear stiffness = $1e8$ N/m
grain contact normal strength= $1e8$ Pa	grain contact shear strength= $1e8$ Pa
grain contact friction coefficient = 0.6	initial porosity = 0.36
wall friction coefficient = 0.6	grain density = 2900 kg/m ³

422

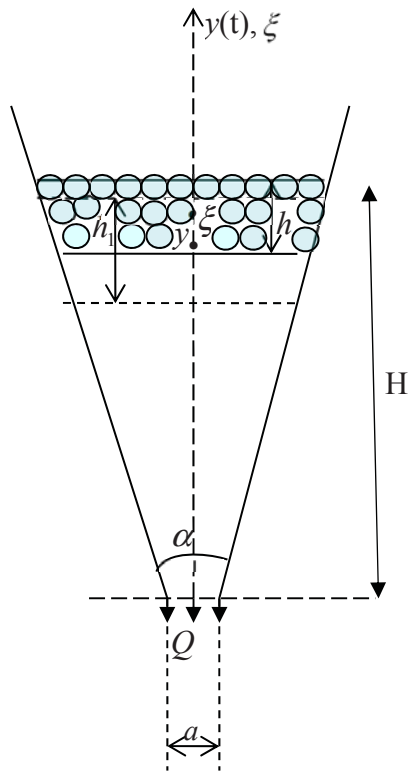


Fig. 1: Schematic diagram of a typical discrete layer of grains used in DLA

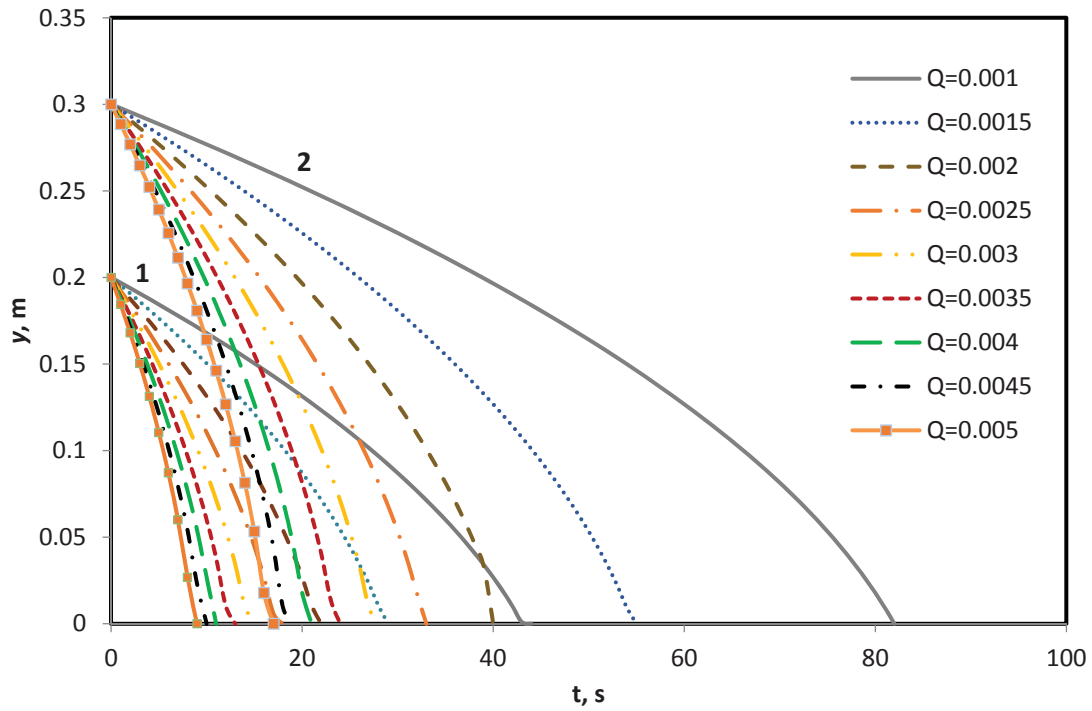


Fig. 2: Location of the top most discrete layer (y in Fig.1) with time (t) under different flow rates Q (m^2/s) (case-1: $H=0.2\text{m}$, case-2: $H=0.3\text{m}$)

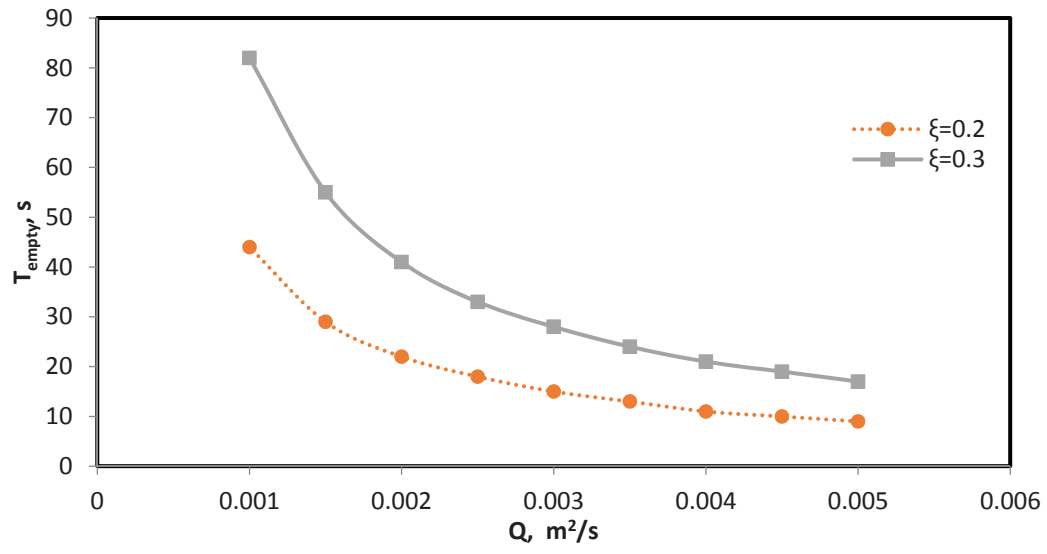


Fig. 3: Variation of the time to empty the hopper with the granular flow rate (Q)

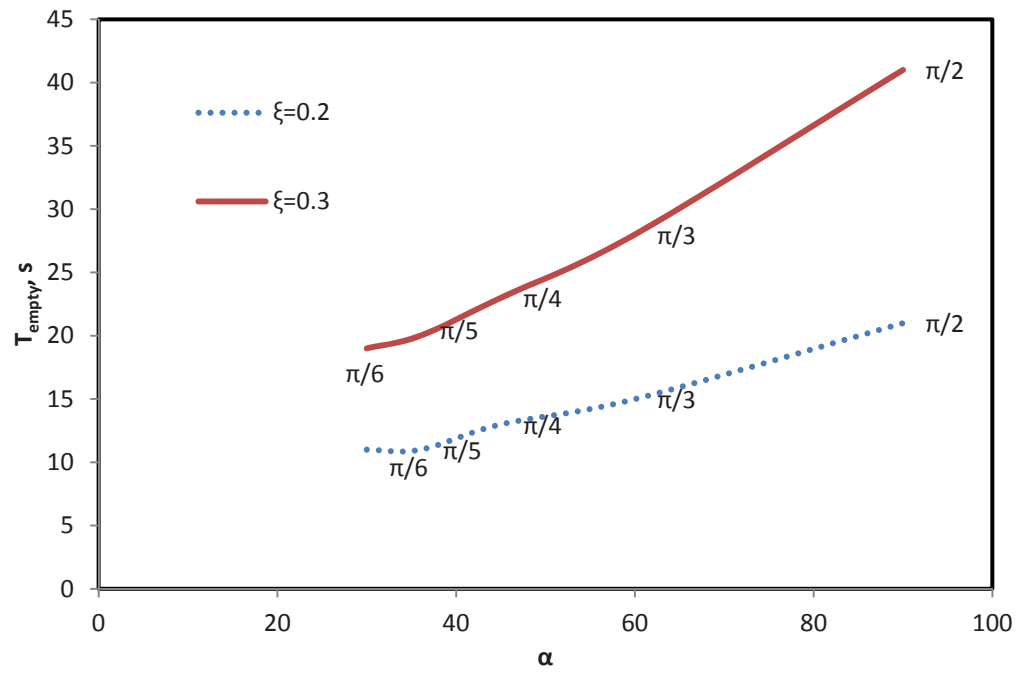


Fig. 4: Time to empty the particles from the hopper in relation to the hopper angle (α)

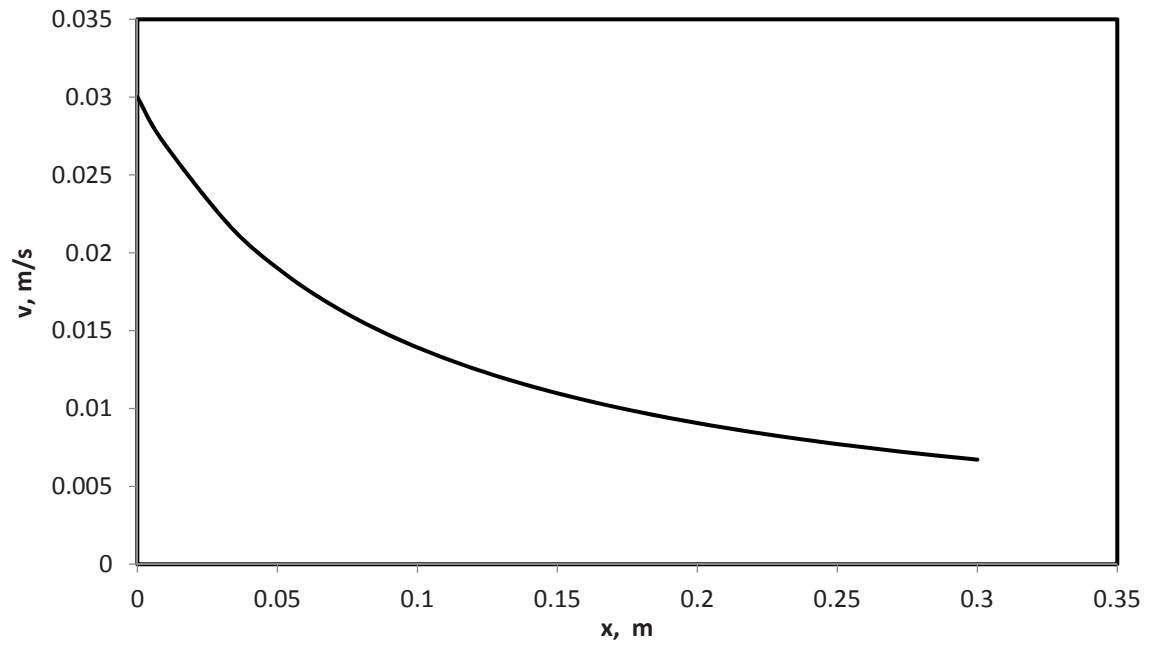


Fig. 5: Variation of the normal velocity of the particles with x ($\xi = 0.3$)

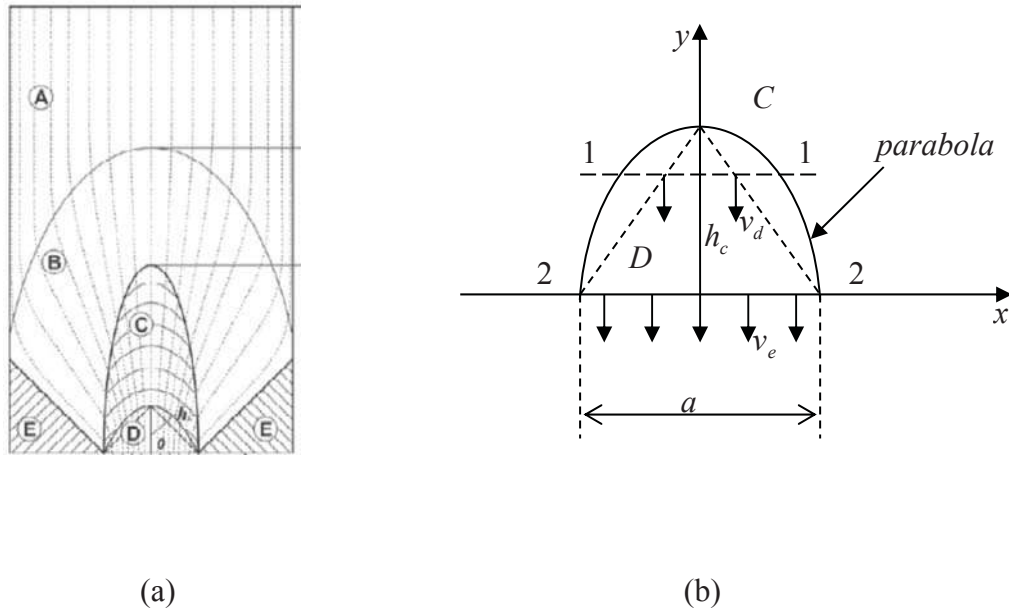


Fig. 6: (a) Zones of flow of the granular particles inside a hopper (Kirya, 2009) (b) expanded diagram of Zone D

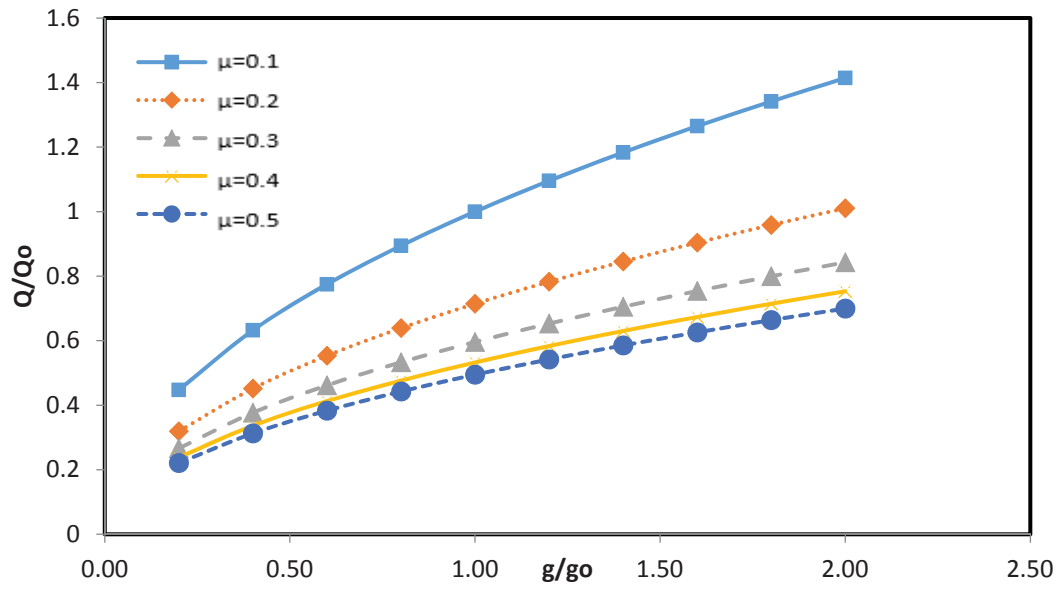
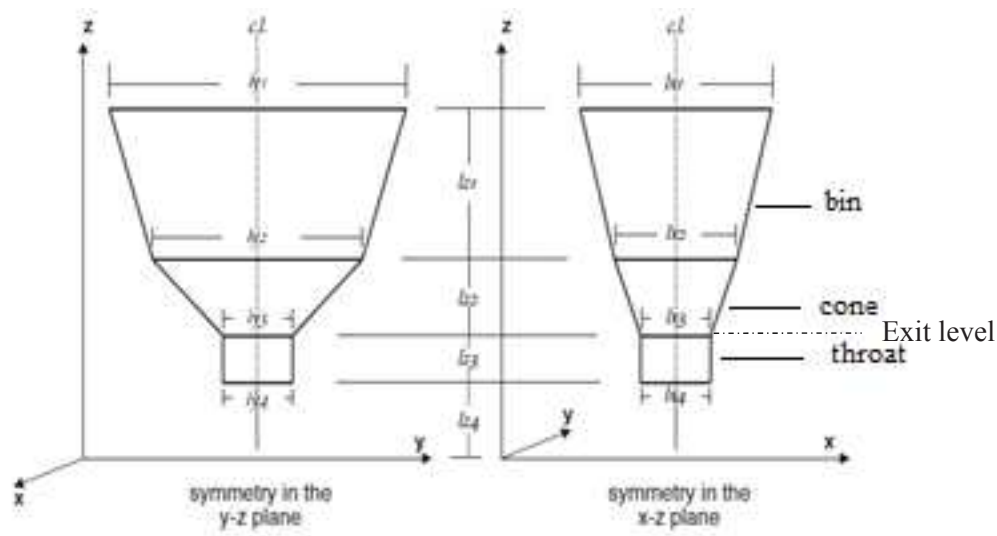
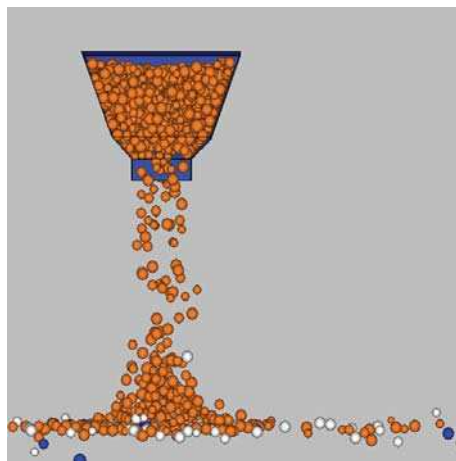


Fig. 7: Effects of friction coefficient and gravity on the granular flow rate using Kirya's structural model



(a)



(b)

Fig. 8: (a) Dimensions of the granular flow container scaled to slit opening width $l_{x4} = l_{y4} = 10$ mm. $l_{x1} = l_{y1} = 35$ mm; $l_{x2} = l_{y2} = 22$ mm; $l_{x3} = l_{y3} = 10$ mm; $l_{x4} = l_{y4} = 10$ mm; $l_{z1} = 18$ mm; $l_{z2} = 4$ mm; $l_{z3} = 4$ mm. (b) a typical snap shot of the flow of sandstone grains from the DEM simulation.

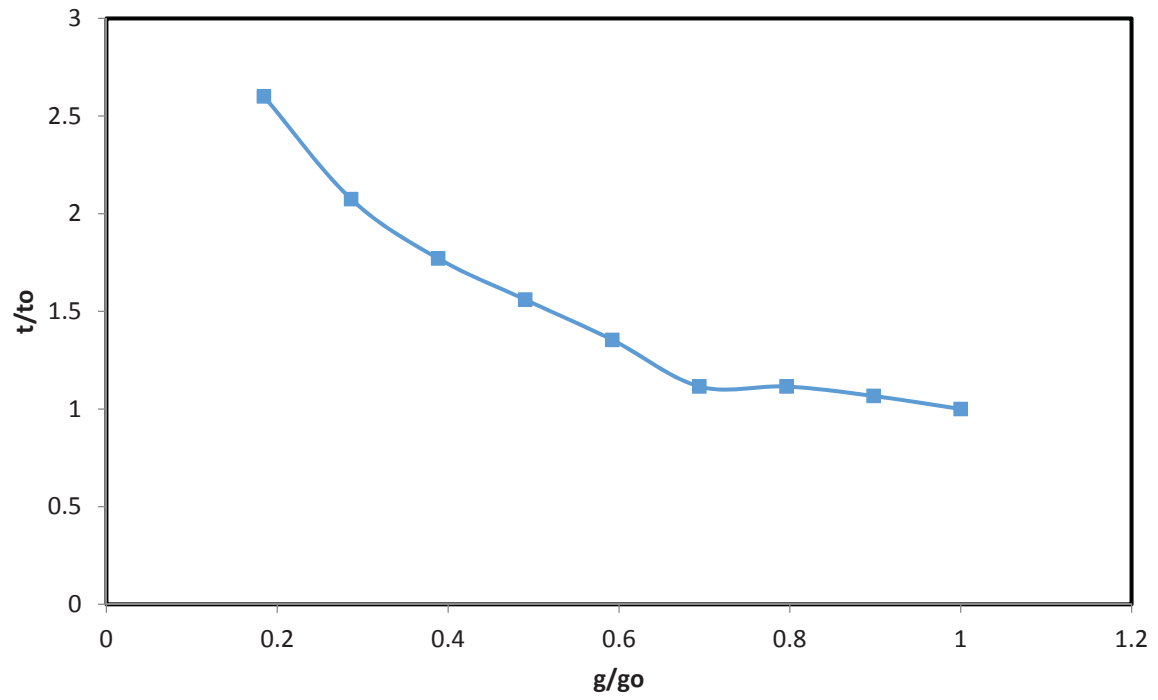


Fig. 9: Variation of the emptying time of the grains with gravity

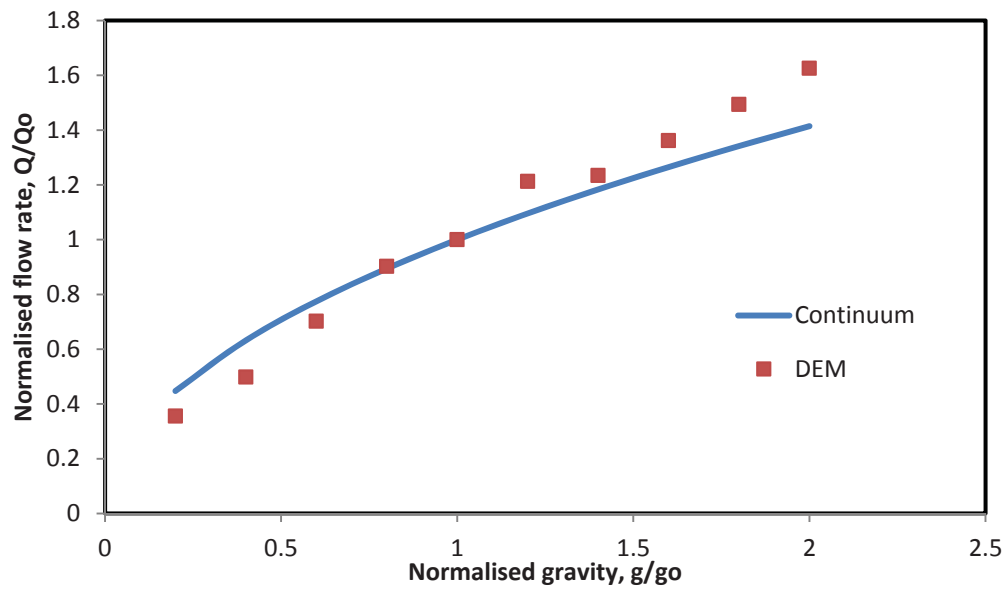


Fig. 10: Comparison of the flow rate (Q) of the sandstone grains obtained from DEM simulations and Kirya's continuum model under different gravity levels (g)

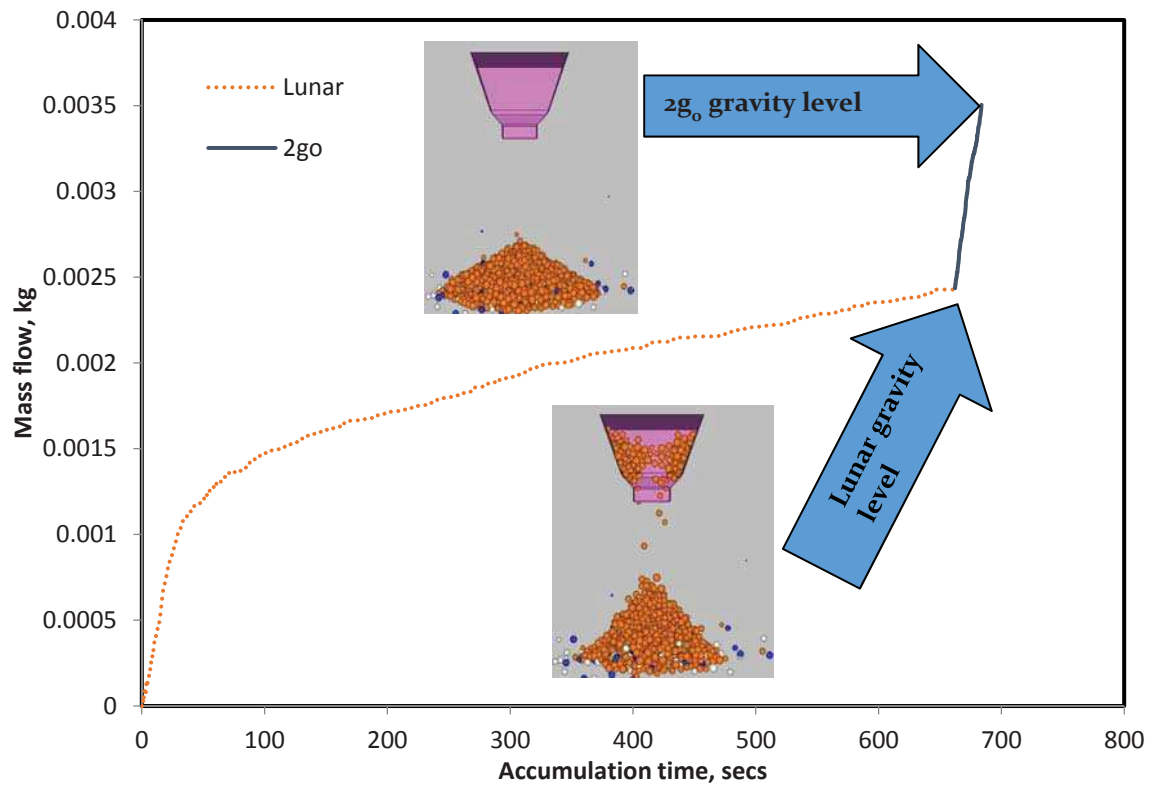


Fig. 11: Mass of sandstone grains exited from the flow chamber under the lunar gravity ($1/6^{\text{th}}$ of g_0) and $2g_0$ gravity levels

FIGURE CAPTIONS

Fig. 1: Schematic diagram of a typical discrete layer of grains used in DLA

Fig. 2: Location of the top most discrete layer (y in Fig.1) with time (t) under different flow rates Q (m^2/s) (case-1: $H=0.2\text{m}$, case-2: $H=0.3\text{m}$)

Fig. 3: Variation of the time to empty the hopper with the granular flow rate (Q)

Fig. 4: Time to empty the particles from the hopper in relation to the hopper angle (α)

Fig. 5: Variation of the normal velocity of the particles with x ($\xi = 0.3$)

Fig. 6: (a) Zones of flow of the granular particles inside a hopper (Kirya, 2009) (b) expanded diagram of Zone D

Fig. 7: Effects of friction coefficient and gravity on the granular flow rate using Kirya's structural model

Fig. 8: (a) Dimensions of the granular flow container scaled to slit opening width $l_{x4} = l_{y4} = 10$ mm. $l_{x1} = l_{y1} = 35\text{mm}$; $l_{x2} = l_{y2} = 22\text{mm}$; $l_{x3} = l_{y3} = 10\text{mm}$; $l_{x4} = l_{y4} = 10\text{mm}$; $l_{z1} = 18\text{mm}$; $l_{z2} = 4\text{mm}$; $l_{z3} = 4\text{mm}$. (b) a typical snap shot of the flow of sandstone grains from the DEM simulation.

Fig. 9: Variation of the emptying time of the grains with gravity

Fig. 10: Comparison of the flow rate (Q) of the sandstone grains obtained from DEM simulations and Kirya's continuum model under different gravity levels (g)

Fig. 11: Mass of sandstone grains exited from the flow chamber under the lunar gravity ($1/6^{\text{th}}$ of g_0) and $2g_0$ gravity levels